

Ab initio Algorithmic Causal Deconvolution of Intertwined Programs and Networks by Generative Mechanism

Hector Zenil^{1,2,3,4}, Narsis A. Kiani^{1,2,3,4}, Jesper Tegnér^{2,3,5}

¹ Algorithmic Dynamics Lab, Centre for Molecular Medicine,
Karolinska Institute, Stockholm, Sweden

² Unit of Computational Medicine, Department of Medicine,
Karolinska Institute, Stockholm, Sweden

³ Science for Life Laboratory, SciLifeLab, Stockholm, Sweden

⁴ Algorithmic Nature Group, LABORES for the Natural and
Digital Sciences, Paris, France

⁵ Biological and Environmental Sciences and Engineering Division,
Computer, Electrical and Mathematical Sciences and Engineering
Division, King Abdullah University of Science and
Technology (KAUST), Kingdom of Saudi Arabia
{hector.zenil, narsis.kiani, jesper.tegner}@ki.se

Abstract

To extract and learn representations leading to generative mechanisms from data, especially without making arbitrary decisions and biased assumptions, is a central challenge in most areas of scientific research particularly in connection to current major limitations of influential topics and methods of machine and deep learning as they have often lost sight of the model component. Complex data is usually produced by interacting sources with different mechanisms. Here we introduce a parameter-free model-based approach, based upon the seminal concept of Algorithmic Probability, that decomposes an observation and signal into its most likely algorithmic generative mechanisms. Our methods use a causal calculus to infer model representations. We demonstrate the method ability to distinguish interacting mechanisms and deconvolve them, regardless of whether the objects produce strings, space-time evolution diagrams, images or networks. We numerically test and evaluate our method and find that it can disentangle observations from discrete dynamic systems, random and complex networks. We think that these causal inference techniques can contribute as key pieces of information for estimations of probability distributions complementing other more statistical-oriented techniques that otherwise lack model inference capabilities.

Keywords: Model generation; signal decomposition; segmentation; algorithmic renormalization; algorithmic image segmentation; graph partitioning; algorithmic machine learning; model generation; feature selection.

1 Introduction

Classical information theory has provided rigorous ways to capture our intuitive notions regarding uncertainty and information, and made an enormous impact in doing so. One of the fundamental measures here is mutual information, which captures the average information contained in one variable about another, and vice versa. If we have two source variables and a target, for example, we can measure the information held by one source about the target, the information held by the other source about the target, and the information held by those sources together about the target. Any other notion about the directed information relationship between these variables, which can be captured by classical information-theoretic measures (e.g., conditional mutual information terms) is linearly redundant with those three quantities.

However, intuitively, there is strong desire to measure further notions of how this directed information interaction may be decomposed, e.g., how much information the two source variables hold redundantly about the target, how much each source variable holds uniquely, and how much information can only be discerned by synergistically examining the two sources together. These notions go beyond the traditional information-theoretic view of a channel serving the purpose of reliable communication, considering now the situation of multiple communication streams converging on a single target. This is a common situation in biology, and in particular in neuroscience, where, say, the ability of a target to synergistically fuse multiple information sources in a non-trivial fashion is likely to have its own intrinsic value, independently of reliability of communication.

The absence of measures for such decompositions into redundant, unique and synergistic information is arguably the most fundamental missing piece in classical information theory. Triggered by the formulation of the Partial Information Decomposition framework by Williams and Beer in 2010, the past few years have witnessed a concentration of work by the community in proposing, contrasting, and investigating new measures to capture these notions of information decomposition.

Typically, models encode features of data in statistical form and in single variables and merged models, even in cases where several data sources are involved. Quantitative measures to disentangle complex signals and methods to tell apart causal mechanisms from noise and (ir)relevant interactions are of broad interest in areas such as statistical mechanics, reverse engineering, network inference, data reconstruction and scientific discovery in general, being germane to the challenge of causal analysis. For example, the

development of techniques for learning disentangled representations using probabilistic machine and deep learning methods has recently gained significant momentum [11]. More broadly, model-based representations from data is one of the main challenges in machine learning, artificial intelligence and causal discovery and inference. Here we introduce a framework based upon the theory of algorithmic probability, which in our formulation is capable of identifying different sources that may explain and provide different models for each of the possible causes of convoluted or intertwined data. Casual inference has been one of the most challenging problems in science. The debate about causality has not prevented the development of successful and mature mathematical and algorithmic frameworks, first in the form of classical statistics and today in the form of computability and algorithmic information theories. Based on these latest mature mathematical frameworks that are acknowledged to fully characterize the concept of randomness as opposed to causal (deterministic), we introduced a suite of algorithms [20] to study the algorithmic information dynamics of evolving systems, and also methods to reduce the dimensions of data [21] based on the same principles. Algorithmic data dimension reduction and algorithmic deconvolution are two challenges which can be viewed as opposite sides of the same coin. On the one hand, data reduction is achieved by finding elements that are considered redundant, using as a criterion their contribution to the algorithmic content of the description of the data. Such elements provide the basis for compression and they can therefore safely be removed. On the other hand, the algorithmic deconvolution by generative mechanisms operates by identifying the elements that are likely to be part of the same causal path of some production rule or generating mechanism. The deconvolution is thus able to decompose causes and pinpoint the different sources generating the observed data.

2 Notation and Background

2.1 Cellular automata

We use cellular automata as causal dynamical systems to illustrate the algorithm before demonstrating its capabilities on more sophisticated objects of a convoluted nature and its applications to objects such as complex networks.

A cellular automaton is a computer program that applies in parallel a global rule composed of local rules on a tape of cells with symbols (e.g. binary). Thoroughly studied in [22], Elementary Cellular Automata (or

ECA) are one-dimensional cellular automata that take into consideration in their local rules the cell next to the centre and the centre cell.

Definition 2.1. A *cellular automaton* (or CA) is a tuple $\langle S, (\mathbb{L}, +), T, f \rangle$ with a set S of states, a lattice \mathbb{L} with a binary operation $+$, a neighbourhood template T , and a local rule f .

The *set of states* S is a finite set with elements s taken from a finite alphabet Σ with at least two elements.

Definition 2.2. The *neighbourhood template* $T = \langle \eta_1, \dots, \eta_m \rangle$ is a sequence of \mathbb{L} . In particular, the neighbourhood of cell i is given by adding the cell i to each element of the template T : $T = \langle i + \eta_1, \dots, i + \eta_m \rangle$. Each cell i of the CA is in a particular state $c[i] \in S$. A *configuration* of the CA is a function $c : \mathbb{L} \rightarrow S$. The *set of all possible configurations* of the CA is defined as $S_{\mathbb{L}}$.

As a discrete dynamic system, the *evolution of the CA* occurs in discrete time steps $t = 0, 1, 2, \dots, n$. The transition from a configuration c_t at time t to the configuration $c_{(t+1)}$ at time $t + 1$ is induced by applying the local rule f . The local rule is to be taken as a function $f : S^{|T|} \rightarrow S$ which maps the states of the neighbourhood cells of time step t in the neighbourhood template T to cell states of the configuration at time step $t + 1$:

$$c_{t+1}[i] = f(c_t[i + \eta_1], \dots, c_t[i + \eta_m]) \quad (1)$$

The general transition from configuration to configuration is called the *global map* and is defined as: $F : S^{\mathbb{L}} \rightarrow S^{\mathbb{L}}$.

In the case of 1-dimensional CA it is common to introduce the *radius* of the neighbourhood template which can be written as $\langle -r, -r + 1, \dots, r - 1, r \rangle$ and has length $2r + 1$ cells. With a given radius r the local rule is a function $f : \mathbb{Z}_{|S|}^{|S|^{(2r+1)}} \rightarrow \mathbb{Z}_{|S|}$ with $\mathbb{Z}_{|S|}^{|S|^{(2r+1)}}$ rules. *Elementary Cellular Automata (ECA)* have a radius $r = 1$ (closest neighbours), having the neighbourhood template $\langle -1, 0, 1 \rangle$, meaning that the neighbourhood comprises a central cell. From this it follows that the rule space for ECA contains $2^{2^3} = 256$ rules.

Enumeration of ECA rules: It is common to follow the lexicographic ordering scheme introduced by Wolfram [22]. According to this encoding, the 256 ECA rules can be encoded by 8-bits.

2.2 Causation and Algorithmic Probability

The concept of algorithmic complexity [5, 2] is at the core of the challenge of complexity in discrete dynamic systems, as it involves finding the most sta-

tistically likely generating mechanism (computer program) that produces a set of given data. Formally, the algorithmic complexity (also known as Kolmogorov-Chaitin complexity) is the length of the shortest computer program that reproduces the data from its compressed form when running on a universal Turing machine.

We used the so-called Coding Theorem (CTM) and Block Decomposition Methods (BDM) as introduced in [3, 9, 13, 19] based on the seminal concept of Algorithmic Probability [10, 6], which in turn is strongly related to algorithmic complexity [5, 2]. However, the algorithm introduced here is independent of the method used to approximate algorithmic complexity such as BDM. BDM assigns an index associated with the size of the most likely generating mechanism producing the data according to Algorithmic Probability [10]. BDM is capable of capturing features in data beyond statistical properties [19, 16] and thus represents an improvement over classical information theory. Because finding the program that reproduces a large object is computationally very expensive— even to approximate— BDM finds short candidate programs using another method [3, 9] that finds and reproduces fragments of the original object and then puts them together as a candidate algorithmic model of the whole object [19, 13]. These short computer programs are effectively model candidates explaining each fragment, with the long finite sequence of short models being itself a generating mechanistic model.

3 Methods and deconvolution algorithm

The aim of the deconvolution algorithm is to break a dataset into groups that do not share certain features (essentially causal clustering and algorithmic partition by probable generative mechanism, completely different from traditional clustering and partition in machine learning approaches). Usually these characteristics are a parameter to maximize, but ultimately the purpose is to distinguish components that are generated similarly from those that are generated differently. In information-theoretic terms the question is therefore as follows: What are the elements (e.g. nodes or edges) that can break a network into the components that maximize their algorithmic information content, that is, those elements that preserve the information about the underlying programs generating the data?

Formally, we seek the edges $\{e_1, \dots, e_n\} \in E_j^* \subset G$ that break G into N disconnected components such that the removal of all edges in E^* minimizes the loss of information in G among all sets E_i^* , i.e. $\langle C(G \setminus E_j^*) \rangle < C(G \setminus E_i^*)$

for all E_i^* .

The algorithm's pseudo-code can thus be written as follows:

1. Find the subset j such that $C(G \setminus E_j^*) < C(G \setminus E_i^*)$ for all subsets $i \in E^*$.
2. Remove the elements in E_j^* .
3. Repeat 1 with $G := G \setminus \{e_j\}$ until N number of subcomponents is reached.

The only parameter that the algorithm would require is the number of desired components into which an object will be decomposed. However, there is a natural way to find the optimal terminating step and therefore the number of maximum possible components that minimize the sum of the lengths of the candidate generating mechanisms.

Before introducing the terminating criterion indicating the number of components, let's analyze what it might mean for two components when $C(s_1) = C(s_2)$. Clearly that subcomponents s_1 and s_2 have the same algorithmic complexity (an integer—or a real value if using AP-based BDM—indicating the size of the approximated minimal program) does not imply that the two components are generated by exactly the same generating mechanism. However, because of the exponential decay of the algorithmic probability of an increasingly random object, we have it that the less random it is, the exponentially more likely it is that the underlying mechanism will be the same. This is because there are exponentially fewer short programs than long ones. For example, in the extreme case of connected graphs, we have it that the complete graph K_n has the smallest possible algorithmic complexity $\sim \log(n)$. So if $C(s_1) = C(s_2) \sim \log(n)$ then s_1 and s_2 are, with extremely high probability, generated by the same algorithm that generates the complete graph (see Fig. 4C). Conversely, if $C(s_1) = C(s_2)$ but $C(s_2)$ and $C(s_1)$ depart from $\log(n)$ (and approximate algorithmic randomness) then the likelihood of being generated by the same algorithm exponentially vanishes. So the information regarding both the algorithmic complexity of the components and their relative size sheds light on the candidate generating mechanisms.

3.0.1 Algorithm terminating criterion

The immediate question is where we should stop breaking down a system into its causal components. The previous section suggests a terminating criterion. Let S be the object which has been produced by N mostly independent generative mechanisms. We decompose S into n parts s_1, \dots, s_n in

such a way that each s_i , $i \in \{1 \dots n\}$ has an underlying generating mechanism found by running the algorithm iteratively for increasing n , but after each iteration we calculate the minimum of the differences in algorithmic complexity among all subcomponents. The algorithm will stop where the number of subcomponents is exactly N , because the sum of the lengths of each of the programs producing more than N components than N will be greater than the length of the single causal mechanisms producing each independent part.

As a trivial example, let's take the string 1^n , where S^n means that the pattern S is repeated n times. After application of the algorithm, the terminating criterion will suggest that 1^n cannot be broken down into smaller segments, each with a different causal generating mechanism, whose total length sums will be shorter than the length of the generating mechanism producing 1^n itself. This is because the sum of the length of the shortest programs $\sum_i |p_i|$ running on a universal Turing machine generating segments of 1^n of length $m_i < n$ each, such that the concatenation $\cup_{i=1} p_i = 1^n$, will be strictly greater than $C(1^n)$, given that each p_i halting criterion will require $i \log m_i$ bits more than $C(1^n)$.

In the case of Fig. 2, the terminating criterion retrieves $N = 3$ components from the two interacting ECA (rule 60 and 110). This does not contradict the fact that we started from two generating mechanisms, because there are three clear regimes that are actually likely to be reproducible by three different generating mechanisms, as suggested by the deconvolution algorithm itself, and as found in [7], where it has been shown that rule 110 can be emulated by the composition of two simpler ECA rules (rules 51 and 118). As seen in Fig. 2, among the possible causal partitions, $N = 2$ successfully deconvolves ECA rule 60 from rule 110 on the first run, with a stronger difference than the difference found between $N = 3$ components when breaking rule 110 into its two different regimes.

4 Numerical experiments, results, and analysis

4.1 Decomposition of sequences and space-time diagrams

In this section, we will test the suggested algorithm on different types of objects, in order to show its applicability and power. We start with the simplest version of an object which conveys information, a string, and move later to consider richer objects such as networks.

We will use different programs to produce different parts of a string, that is a program p to generate segment s_1 and program p' to generate segment

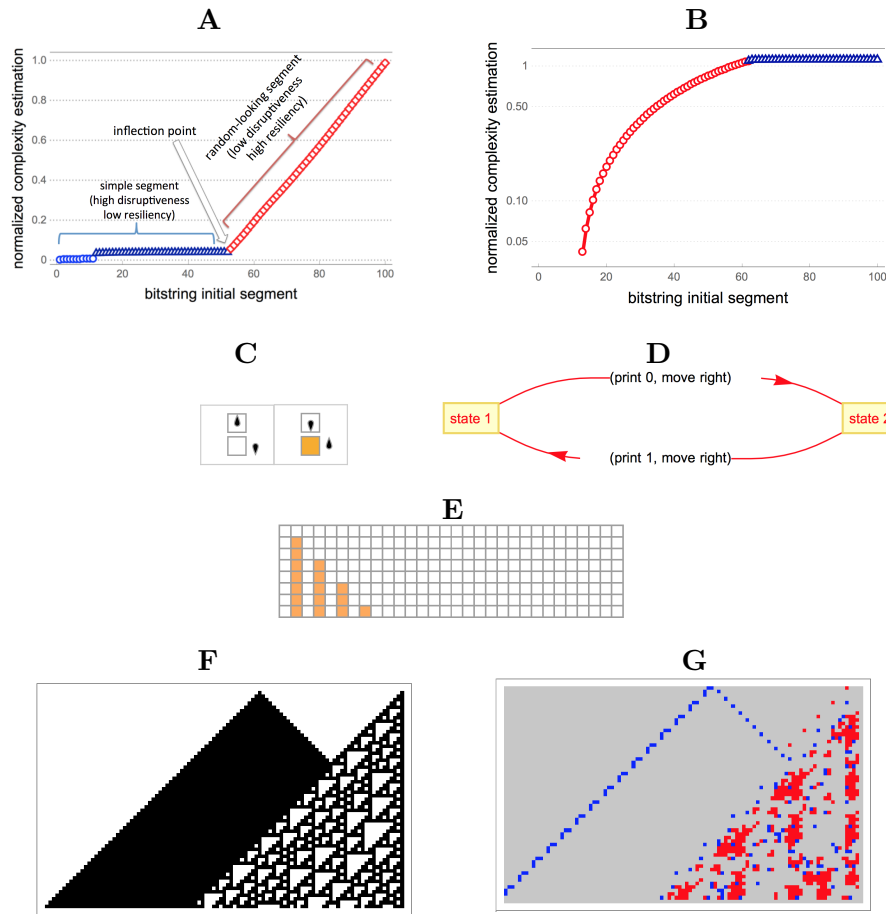


Figure 1: Proof of concept applied to a binary string composed of two segments with different underlying generating mechanisms (computer programs). A: Log plot of complexity estimation of a regular segment (blue) consisting of the repetition of ‘01’ 25 times followed by a random-looking segment (red). B: Log plot reversing the order of A yet preserving the qualitative behaviour of the different segments. C: The code of the smallest generating program (a non-terminating Turing machine) depicted visually (states are arrows in different directions) producing the string of 01^n for any n (0 is white and 1 is orange) starting from a blank tape as shown in the space-time diagram (E). D: the same computer program as a state diagram. F: Interacting programs with different generating mechanisms (ECA rules 255 v 110) running for 60 steps. G: Algorithmic information footprint, every pixel is deleted and its original contribution to the whole quantified and coloured accordingly. If grey, then it makes the lowest contribution, blue represents a low contribution and red the highest contribution (randomness).

repeated any number of times n , the length of the computer program is of (almost) fixed size, growing only by $\log(n)$ if the computer program is required to stop after n iterations. In this case 01^n is a trivial example with a strong statistical regularity whose low complexity could be captured by applying Shannon entropy alone on blocks of size 2.

Figs. 1 F and G illustrate how the algorithm can separate regions produced by generating mechanisms of different algorithmic information content by observing their space-time dynamics, thereby contributing to the deconvolution of regions that are produced by different generating mechanisms. In this example both programs are sufficiently robust to not break down (see Sup. Inf.) when they interact with each other, with rule 110 prevailing over 255. Yet, in the general case it is not always easy to tell these mechanisms apart. In more sophisticated examples such as in Figs. 2 D to E, we see how the algorithm can break down contiguous regions separating an object into two major components corresponding to the different generating computer programs that are intertwined and actively interacting with each other. The experiment was repeated 20 times with programs with differing qualitative (e.g. Wolfram class) behaviour.

Fig. 2 F demonstrates that perturbations to regions in red are considered to have a more random effect and are thus by themselves less algorithmically complex (random) versus simple. When regions are of the same algorithmic complexity they are likely to be generated by similar algorithms, or more precisely, algorithms that are of similar minimal length. Regions in blue move the space-time evolution away from randomness and are themselves more algorithmically random. Blue structures on the left hand side correspond to large triangles occurring in ECA rule 110 that are usually used to compute and transfer information in the form of particles. However, triangular patterns transfer information in a limited way because their light cone of influence reduces at the greatest possible speed of the automaton, and they are assigned an absolute neutral information value. Absolute neutral values are those closest to 0. Once separated, the two regions have clearly different algorithmic characteristics given by their causal perturbation sensitivity, with the right hand side being more sensitive to both random and non-random perturbations. Moreover, Fig. 2 F shows results compatible with the theoretical expectation and findings in [20] where a measure of reprogrammability associated with the number and magnitude of elements that can move a dynamical system towards or away from randomness was introduced and shown to be related to fundamental properties of the attractor space of the system.

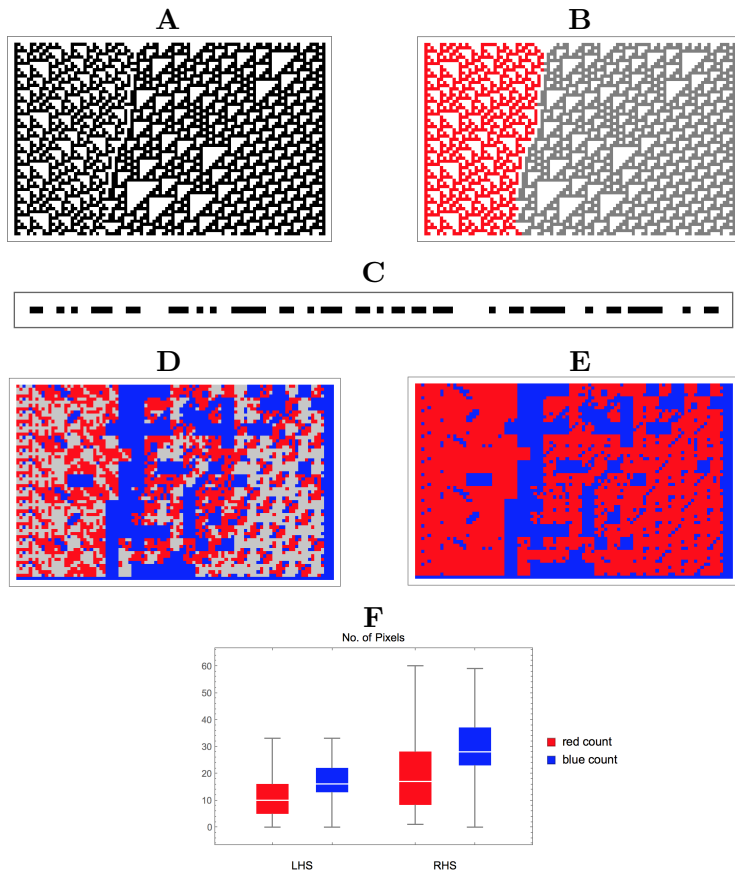


Figure 2: A: The output of two different intertwined programs (ECA rules 60 and 110) with qualitatively complex output behaviour (11 to 60 steps depicted here, from a random initial condition) interacting with each other (one of which has been proven to be Turing-universal and the other has also been conjectured to be universal [22]), each producing structures of a similar type that, from an observer’s perspective, are difficult to distinguish (see Subfigure C) as is artificially done in B (knowing which pixel is generated by which rule). C: What an observer of the last runtime would see in the form of a stream of bits with no clear statistical distinction. D: The algorithm pinpoints the regions of neutral, positive and negative, with the contiguous largest blue component segmenting the image into two components. E: only negative vs positive causal contributions where both Shannon entropy and a popular lossless compression algorithms fail (see SI). F: Sanity check/validation: Statistically significant quantitative differences among the parts after application of the algorithm as illustrated in E among apparently weak qualitative differences as illustrated in Subfig. A.

4.2 Graph and network deconvolution

Classification can usually be viewed as solving a problem which has an underlying tree structure according to some measure of interest. One way to think of optimal classification is to discover a tree structure at some level of depth, with tree leaves closer to each other when such objects have a common or similar causal mechanism and for which no feature of interest has been selected. Fig. 3 illustrates how the algorithm may data, in this case starting from a trivial example that breaks complete K -ary trees. Traditionally, partitioning is induced by an arbitrary distance measure of interest that determines the connections in a tree, with elements closer to a cluster centre connected by edges. The algorithm breaks the trees (see Fig. 3) into as many components as desired by iterating the algorithm until the number of desired components is obtained or the terminating criterion is applied (c.f. Subsection 3.0.1). Figs. 3A,B provide examples illustrating how to maximize topological symmetry. The algorithm can be applied, without loss of generalization, to any non-trivial graph, as in Figs. 3C,D or on any dataset for that matter.

The same task using classical information theory (Shannon entropy) is shown not to be sensitive enough (see Sup. Inf.), and a popular lossless compression algorithm (Compress based on LZW) provided a noisy approximation (see Sup. Inf.) to the results obtained by using the Block Decomposition Method, as defined in [19], whose description is provided in the Sup. Inf.

Figs. 3C-E illustrate how randomly connected graphs with different topologies can be broken into their respective generative mechanisms. Fig. 3C is a complete graph of size 20 randomly connected by 3 edges to a scale-free graph of size 100. The graphs are generated by different mechanisms, one is a small program that, given a number N of nodes, produces a graph with all nodes connected to all other $N - 1$ nodes and has a program of small length that grows only by $\log N$ [15]. The scale-free network is generated by the canonical preferential attachment algorithm with two edges per node and requires a slightly longer algorithm that grows by $\log N + c$ [15] where c is a small constant accounting for the pseudo-random choice of attachment nodes. The algorithm breaks the graphs into two components, each of which corresponds to the graphs with different degree distribution (depicted below each case) associated with its generating mechanism. This is because $|P(G_1)| + |P(G_2)| + \dots + |P(G_n)| + |P(e_{G_i})| > |P(G_1 G_2 \dots G_n)|$ for any G_i , where e_{G_i} is the set of edges randomly connecting G_i to G_j for any i and j for all G of low algorithmic complexity.

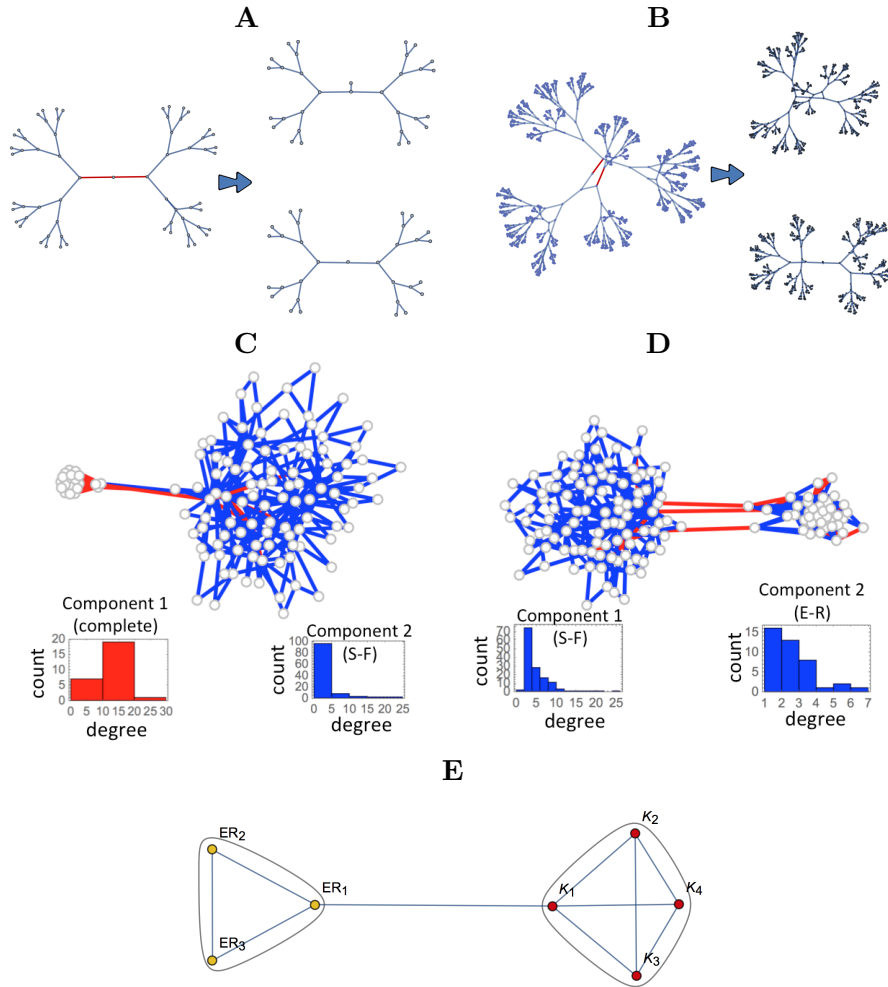


Figure 3: A,B: Forced deconvolution of a tree to minimize the graph algorithmic information loss among the resulting components by maximizing causal resemblance of components (causal clustering) (see Terminating criterion Subsection). Depicted are K -ary trees of size 6 (A) and 10 (B) and their resulting graphs after a single application. C: Deconvoluting/separating a graph composed by a complete graph and a scale-free (S-F) network generated by preferential attachment and randomly connected between them. Negative edges break down the graph into components corresponding to the different underlying generating mechanisms. D: Deconvolution of a random graph (E-R) and a scale-free (S-F) network. E: The algorithm first separates the subcomponents with the largest algorithmic difference, followed by other subcomponents.

4.3 Robustness and limitations

Fig. 3 D illustrates a similar case to Fig. 3 C, but instead of a complete graph an Erdős Rényi (E-R) graph with edge density 0.5 is produced and connected by 3 random edges to a scale-free network produced in the same fashion as in Fig. 3 C. Again, the algorithm was able to break it down into the two corresponding subgraphs. Fig. 3 D represents a test case to evaluate the effect of additive noise by connecting an E-R graph of increasing size and with an increasingly greater number of random edges.

Next we ask how much structure, if any, can be recovered/extracted when adding a random (E-R) graph to different types of structured networks. To this end, we conducted a series of numerical experiments shedding light on the limitations of the algorithm introduced here in the face of additive noise. The same results were obtained for the simpler case of connecting any complete graph of increasing size to any other graph such as E-R or S-F.

Fig. 4 shows the results from the experiments separating graphs, in this case a scale-free graph (S-F) from an Erdős Rényi graph (E-R), the former generated by a Barábasi-Albert preferential attachment algorithm [1] and the latter produced by a pseudo-random generator. Fig. 4A quantifies the error and optimal signal-to-noise ratio for optimal deconvolution, testing the algorithm under additive noise both for fixed and growing size subcomponents. Fig. 4B shows links coloured in red as identified by the algorithm having the highest algorithmic information value when their removal sends the original composed system towards lower algorithmic information content, thereby telling apart the two subcomponents. Negative links are mostly on the side of the E-R graph. In other words, the S-F can be extracted with the greatest precision and a lower rate of false positives from the mix, which is to be expected given the random nature of the added links that connect the graphs, making them more like the E-R links than the S-F. If only the number of random links among graphs increases for fixed size graphs (Fig. 4B blue circle marks) a maximum precision of about 0.9 is reached before degradation. That is, at around 32.5% of the links randomly connecting the components. In other words, the algorithm is robust, telling apart noise from structure even after up to 0.325 (from the random links connecting the components) $+ 0.5$ (from the E-R component) $= 0.825$, i.e. 82.5% of all links are random. On the other hand, the number of false positives is constant at about 5%, in the case shown in Fig. 4B all of the false positives (red links not connecting the two graphs with different topology) are inside the E-R graph and mostly nonexistent on the side of the less random S-F graph.

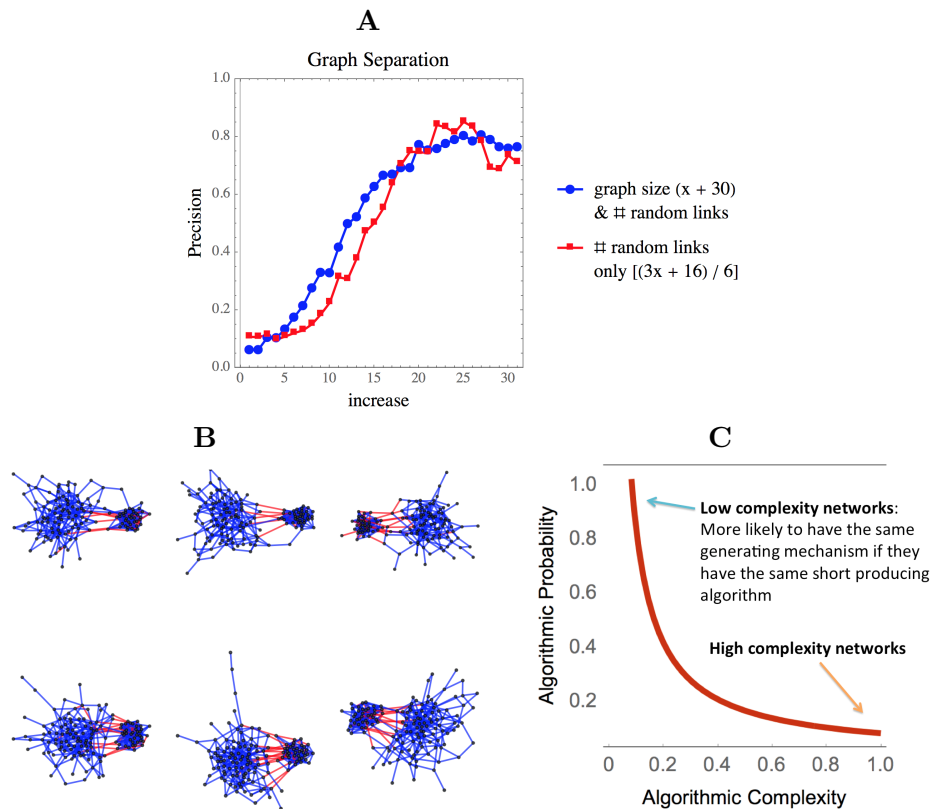


Figure 4: A: Causal deconvolution of graphs, a S-F graph (2 new links per added node) from an E-R (0.5 edge density) graph emulating noise (each point represents the average of 10 replicates). When the number of links increases as a function of the subgraph sizes, the separability is robust (red square markers) compared to increasing the number of random links only for graphs of fixed size (40 nodes), when successful separation is compromised, noise (E-R) and structure (S-F) being indistinguishable. B: A small sample of 6 graphs among the $10 \times 20 = 200$ graphs randomly connecting a S-F to an E-R graph. Success at identifying randomly connecting links is shown and was found to be very robust. C: Objects have exponentially greater chances of being produced by the same generating mechanism if they are of low algorithmic randomness and thus of high algorithmic probability.

5 Remarks and conclusions

For some more sophisticated yet successful examples on which these new algorithmic methods may outperform applications of entropy in general (without access to true probability distributions) and other computable measures see [19], and [16] for a non-trivial example in which entropic measures fail (by offering divergent descriptions of the same evolving system). The generation of these models is key in our approach because the integer (or real) value assigned to a system as an estimation of its algorithmic complexity is nothing but a guiding index of the number of specific models found by our method that are capable of explaining and generating the data.

One possible objection is that any number of interacting rules can be thought of as a single rule producing an intertwined output because we know from Turing universality that any number of interacting programs can also be rewritten as a single program in a larger rule space (defined by state \times symbol) incorporating all the behaviours together. That is, any computer program can be decomposed into one or more computer programs producing the same output. This means that separating programs and signals is, in some way, not fundamental. Fig. 2C-F shows, for example, that by iterating the deconvolution algorithm not only do the two main components of the image correspond to the two generating ECA rules, but a second application of the algorithm would produce a third or more components corresponding to further resilient features generated by the rules, which can be considered rules themselves within a smaller rule (state/symbol) space. However, in the deconvolved observations the interacting rule determining how two or more rules may interact effectively constitutes a third global rule to which the algorithm has no direct access or an apparent region in the observed window.

We have introduced and tested a parameter-free algorithm for causal deconvolution of interlaced and interacting mechanisms using fundamental concepts drawn from the theory of Algorithmic Probability and Algorithmic Information Theory. Our approach enables a parameter-free analysis of the deconvolution problem, since we have removed the need for pre-defined user-centric definitions of global properties or local rules (e.g. distance metrics) to determine the algorithm. Instead, relating our algorithm to the algorithmic information theory provides us with a fundamental metric. While the algorithm uses state-of-the-art algorithms to approximate algorithmic complexity (CTM and BDM), the algorithm and methods introduced here are independent of the approximating method chosen (e.g. lossless compression). However, the precision and accuracy is not. Yet, the algorithm

is sufficiently robust to disentangle sophisticated intertwined causal mechanisms. This opens the possibility of parlaying these algorithmic methods into a more elaborate machine learning framework. For example, the extracted causal information can be used as a prior distribution for machine and deep learning techniques. This is useful because efficient techniques for pattern recognition are as a rule weak on inferring models, and thus ill-equipped to capture the underlying generative mechanisms and thereby produce predictive and prescriptive causal models that exceed the descriptive nature of current classical and modern statistical approaches.

Acknowledgements

H.Z. acknowledges the support of the Swedish Research Council (Vetenskapsrådet) grant No. 2015-05299.

References

- [1] R. Albert, A.-L. Barabási, Statistical mechanics of complex networks, *Reviews of Modern Physics*, 74 (1): 47–97, 2002.
- [2] G.J. Chaitin. On the length of programs for computing finite binary sequences *Journal of the ACM*, 13(4):547–569, 1966.
- [3] J.-P. Delahaye and H. Zenil, Numerical Evaluation of the Complexity of Short Strings: A Glance Into the Innermost Structure of Algorithmic Randomness, *Applied Mathematics and Computation* 219, 63–77, 2012.
- [4] E. Hermo-Reyes and J.J. Joosten, “Competing Cellular Automata” <http://demonstrations.wolfram.com/CompetingCellularAutomata/>, Wolfram Demonstrations Project, June 17, 2014.
- [5] A.N. Kolmogorov. Three approaches to the quantitative definition of information, *Problems of Information and Transmission*, 1(1):1–7, 1965.
- [6] L.A. Levin. Laws of information conservation (non-growth) and aspects of the foundation of probability theory, *Problems of Information Transmission*, 10(3):206–210, 1974.

- [7] J. Riedel and H. Zenil, Rule Primality and Compositional Emergence of Turing-universality from Elementary Cellular Automata, forthcoming, 2017. XXX
- [8] F. Soler-Toscano, H. Zenil, J.-P. Delahaye and N. Gauvrit, *Correspondence and Independence of Numerical Evaluations of Algorithmic Information Measures*, Computability, vol. 2, no. 2, pp. 125–140, 2013.
- [9] F. Soler-Toscano, H. Zenil, J.-P. Delahaye and N. Gauvrit, *Calculating Kolmogorov Complexity from the Frequency Output Distributions of Small Turing Machines*, PLoS One 9(5), e96223, 2014.
- [10] R.J. Solomonoff, A formal theory of inductive inference: Parts 1 and 2. *Information and Control*, 7:1–22 and 224–254, 1964.
- [11] N. Siddharth, B. Paige, J-W van de Meent, A. Desmaison, N.D. Goodman, P. Kohli, F. Wood, P.H.S. Torr, Learning Disentangled Representations with Semi-Supervised Deep Generative Models, arXiv:1706.00400 [stat.ML], 2017.
- [12] H. Zenil, F. Soler-Toscano, K. Dingle and A. Louis, Graph Automorphisms and Topological Characterization of Complex Networks by Algorithmic Information Content, *Physica A: Statistical Mechanics and its Applications*, vol. 404, pp. 341–358, 2014.
- [13] H. Zenil, F. Soler-Toscano, J.-P. Delahaye and N. Gauvrit, *Two-Dimensional Kolmogorov Complexity and Validation of the Coding Theorem Method by Compressibility*, 2013.
- [14] H. Zenil, N.A. Kiani and J. Tegnér, Quantifying Loss of Information in Network-based Dimensionality Reduction Techniques, *Journal of Complex Networks* 4, 342–362, 2016.
- [15] H. Zenil, N.A. Kiani and J. Tegnér, Methods of Information Theory and Algorithmic Complexity for Network Biology, arXiv:1401.3604, 2014.
- [16] H. Zenil, N.A. Kiani and J. Tegnér, Low-Algorithmic-Complexity Entropy-deceiving Graphs, *Physics Reviews E*. 96, 012308, 2017.
- [17] H. Zenil, Compression-based Investigation of the Dynamical Properties of Cellular Automata and Other Systems, *Complex Systems*, 19(1), pages 1–28, 2010.

- [18] H. Zenil and E. Villarreal-Zapata, Asymptotic Behaviour and Ratios of Complexity in Cellular Automata Rule Spaces, *International Journal of Bifurcation and Chaos*, vol. 13, no. 9, 2013.
- [19] H. Zenil, S. Hernández-Orozco, N.A. Kiani, F. Soler-Toscano, A. Rueda-Toicen, A Decomposition Method for Global Evaluation of Shannon Entropy and Local Estimations of Algorithmic Complexity, arXiv:1609.00110 [cs.IT], 2016.
- [20] H. Zenil, N.A. Kiani, F. Marabita, Y. Deng, S. Elias, A. Schmidt, G. Ball, J. Tegnér, An Algorithmic Information Calculus for Causal Discovery and Reprogramming Systems, 2017. BioArXiv DOI: <https://doi.org/10.1101/185637>
- [21] H. Zenil, N.A. Kiani, J. Tegnér, Data Reduction and Network Sparsification by Minimal Algorithmic Information Loss, arXiv XXX
- [22] S. Wolfram, *A New Kind of Science*, Wolfram Media, Champaign IL., 2002.

Supplementary Information

5.1 Interacting programs

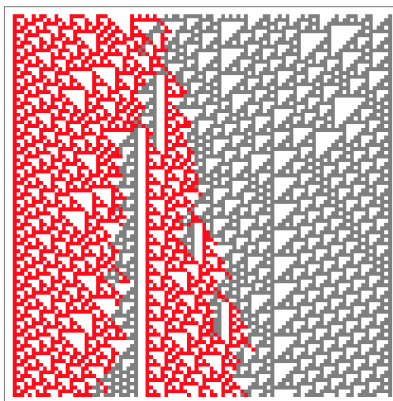


Figure 5: Interacting programs such as cellular automata require us to define how the interaction happens by, e.g., deciding what set of rules apply at the intersection. For instance, one of the two sets of local rules or a 3rd set of rules effectively defining a super cellular automaton that most likely is another cellular automaton in a larger rule-space (requiring more states to define the two sub-cellular automata and the interaction). Depicted here is the type of interaction we explored, and this case shows the richness of such possible interactions where both rules ‘spill over’ each other.

The qualitative behaviour of each program can heuristically be identified by what is known as its Wolfram class, which in turn has been formalized using tools and methods from algorithmic complexity in [17, 18]. Informally, Wolfram class 1 represents evolutions of programs that converge to a simple fixed configuration, exemplars of Wolfram class two converge to repetitive simple behaviour, those of Wolfram class 3 produce unbounded apparently statistically random behaviour and exemplars of Wolfram class 4 reproduce apparently open-ended persistent structures. None of what has been introduced here depends on this behavioural characterization based on different heuristics, and it is thus in no way fundamental to the results reported.

The interaction rule is interaction rule number 1 according to the enumeration open-source program on the Wolfram Demonstrations website publicly available at <http://demonstrations.wolfram.com/CompetingCellularAutomata/> [4] determining the way in which the local rules from each global ECA rule will

be dictated and applied at their intersection.

5.2 Graph generation

The graphs used throughout this paper were generated using the Wolfram Language on the Mathematica platform using the function `RandomGraph[]` with uniform distribution (`UniformGraphDistribution[]`) for Erdős-Rényi graphs and a scale-free distribution (`BarabasiAlbertGraphDistribution[]`) for the scale-free networks constructed by starting from a cycle graph of size 3 and a vertex of k edges added at each step according to the preferential attachment algorithm [1] following a distribution proportional to the vertex degree. All experiments were replicated and averaged from a set of at least 20 instances.

5.3 Comparison with entropy and lossless compression

Fig. 6 shows the results obtained by using classical information theory (Shannon entropy) and one of the most popular lossless compression algorithms (`Compress`) based on LZW as an approximation to algorithmic (Kolmogorov-Chaitin) complexity instead of BDM. Because all values collapse into a single value for entropy, the colours displayed are the result of an artificial sorting of the pixels based on their indices, from top to bottom. Compression is a lower-quality approximation of what we reported in Figs. 1C-F, where the reported algorithm based on the BDM is clearly an improvement.

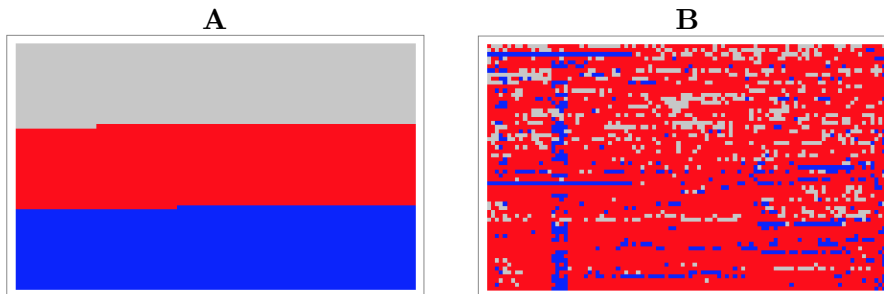


Figure 6: Shannon entropy (A) and lossless compression (`Compress`) underperform, not being sensitive enough in performing the same task reported in Figs. 1C-F.